

Project Report
On
**PERFORMANCE OF A WIND DRIVEN DOUBLY FED
INDUCTION GENERATOR UNDER BALANCED AND
UNBALANCED CONDITION**

Submitted in partial fulfillment of the requirements for the award of the
degree of Master of Engineering (Power System) in Electrical Engineering

of

Gauhati University

Session: 2015-17



By

CHAMPAK KUMAR DAS (PG-E-15/14)

M.E. 3RD SEMESTER

Under the guidance of

Dr. RUNUMI SARMA

Professor

Deptt. of Electrical & Instrumentation Engineering

Assam Engineering College

Department of Electrical & Instrumentation Engineering

Assam Engineering College, Jalukbari, Guwahati

Assam -781013

Certificate from the supervisor

This is to certify that the project report entitled “**Performance of a wind driven Doubly Fed Induction Generator under balanced and unbalanced condition**” has been carried by Champak Kumar Das, ME 3rd Semester under my guidance and is submitted in partial fulfillment of the requirements for the award of the degree of Master of Engineering (Power System) in Electrical Engineering of Gauhati University.

Date:

Place: Guwahati

Dr. Runumi Sarma

Professor

Deptt. of Electrical & Instrumentation Engineering

Assam Engineering College

Certificate from the Head of the Department

This is to certify that the project report entitled “**Performance of a wind driven Doubly Fed Induction Generator under balanced and unbalanced condition**” has been submitted by Champak Kumar Das, ME 3rd Semester in partial fulfillment of the requirements for the award of the degree of Master of Engineering (Power System) in Electrical Engineering of Gauhati University.

Date:

Place: Guwahati

Dr. D. Agarwal

Professor & Head of the Department

Deptt. of Electrical & Instrumentation Engineering

Assam Engineering College

ACKNOWLEDGEMENTS

The satisfaction and euphoria that accompany the successful completion of any task would be incomplete without the mentioning of the people whose constant guidance and encouragement made it possible.

I express my earnest gratitude to my project guide Dr. Runumi Sarma, Professor, Department of Electrical Engineering, for her constant support, encouragement and guidance. I am grateful for her cooperation and her valuable suggestions.

I would also like to express my gratitude to all other members who are involved either directly or indirectly for the completion of this project.

Finally, I am also thankful to the Head of the Electrical and Instrumentation department for his valuable suggestions, co-operation and help.

Champak Kumar Das
ME 3rd Semester
Roll No. PG-E-15/14
Deptt. of Electrical Engineering
Assam Engineering College

ABSTRACT

Wind electrical power systems are recently getting lot of attention, because they are cost competitive, environmental clean and safe renewable power source, as compared with fossil fuel and nuclear power generation. A special type of induction generator, called a doubly fed induction generator (DFIG), is used extensively for high-power wind applications. They are used more and more in wind turbine applications due to ease in controllability, high energy efficiency and improved power quality.

This project aims to develop a method of a field orientation scheme to control both the active and reactive powers of a DFIG driven by a wind turbine. The control system consists of a wind turbine that drives a DFIG connected to the utility grid through AC-DC-AC link. The main control objective is to regulate the dc link voltage for operation at maximum available wind power. This is achieved by controlling the d^e and q^e axes components of voltages and currents for both rotor side and line side converters using PI controllers. The complete dynamic model of the system is described in details. Computer simulations have been carried out in order to validate the effectiveness of the proposed system during the variation of wind speed.

Generally, any abnormalities associated with grid asymmetrical faults affect the system performance considerably. During grid faults, unbalanced currents cause negative effects like overheating problems and mechanical stress due to high torque pulsations that can damage the rotor shaft, gearbox or blade assembly. Therefore, the dynamic model of the DFIG, driven by a wind turbine during grid faults has been analyzed and developed using the method of symmetrical components. The dynamic performance of the DFIG during unbalanced grid conditions is analyzed and described in detail using matlab simulations.

CONTENTS

	Page No.
ABSTACT	i
LIST OF FIGURES	iii
LIST OF TABLES	iv
CHAPTER 1. INTRODUCTION	1
CHAPTER 2. CONTROL OF DOUBLY FED INDUCTION GENERATOR DRIVEN BY WIND TURBINE	4
2.1 Field oriented control of Induction machine	4
2.1.1 Direct field oriented control	7
2.1.2 Indirect field oriented control	9
CHAPTER 3. DYNAMIC MODELLING OF DFIG	10
3.1 Turbine model	10
3.2 DC link model	11
3.3 Complete system model	12
3.4 Field oriented control of DFIG	13
3.5 Complete system configuration	15
3.6 Wind power model	18
CHAPTER 4. DYNAMIC PERFORMANCE OF DFIG DURING UNBALANCED GRID CONDITION	21
4.1 Dynamic model of a DFIG system	21
4.2 Mathematical model of DFIG system under unbalanced grid voltage	23
4.3 System description	27
CHAPTER 5. SIMULINK MODEL, SIMULATION RESULTS AND DISCUSSION	28
5.1 Simulink model	28
5.2 Results and discussion	30
CHAPTER 6. CONCLUSIONS	35
REFERENCES	36

LIST OF FIGURES

Figure	Particulars	Page No.
2.1	Doubly fed wound rotor induction generator driven by a wind turbine	4
2.2	General structure of a field oriented control in a synchronous reference frame for an Induction machine	6
2.3	Structure of a direct field oriented control of a wind driven DFIG	8
2.4	Structure of indirect field oriented control of a wind driven DFIG	9
3.1	Wind turbine control system	10
3.2	Power flow through dc-link element	12
3.3	Control scheme of the DFIG driven by a wind turbine based on field orientation control	17
3.4	Wind Power C_p Curves	19
4.1	Equivalent circuit of a DFIG in the synchronous reference frame rotating at a speed of ω_s	22
4.2	Relationships between the $(\alpha-\beta)$ reference frame and the $(d-q)^+$ and $(d-q)^-$ reference frames	24
4.3	DFIG driven by a wind turbine based on field orientation control during grid fault conditions	27
5.1	Simulink model for normal operation of the DFIG system	28
5.2	Simulink model of DFIG system during unbalanced network condition	29
5.3	Simulation result under normal operation	30
5.4	Simulation result during voltage sag	31
5.5	Simulation result during three phase fault	33

LIST OF TABLES

Table	Particulars	Page No.
3.1	Parameters and data specifications of the DFIG system	18
3.2	Cp coefficients $\alpha_{i,j}$	20

CHAPTER 1

INTRODUCTION

Electrical power is the most widely used source of energy for the homes, work places and industries. Population and industrial growth have led to significant increase in power consumption over the past three decades. Natural resources like coal, petroleum and gas that have driven the power plants, industries and vehicles for many decades are becoming depleted at a very fast rate. This serious issue has motivated nations across the world to think about alternative forms of energy which utilize inexhaustible natural resources.

The combustion of conventional fossil fuel across the globe has caused increased level of environmental pollution. Several international conventions and forums have been setup to address and resolve the issue of climate change. These forums have motivated countries to form national energy policies dedicated to pollution control, energy conservation, energy efficiency, development of alternative and clean sources of energy.

Renewable energy sources like solar, wind, and tidal are sustainable, inexhaustible, environmental friendly and clean energy sources. Due to all these factors, wind power generation has attracted great interest in recent years. Undoubtedly, wind power is today's most rapidly growing renewable energy source. Even though the wind industry is young from a power systems point of view, significant strides have been made in the past 20 years. Increasing reliability has contributed to the cost decline with availability of modern machines reaching 97-99%. Wind plants have benefited from steady advances in technology made over past 15 years. Much of the advancement has been made in the components dealing with grid integration, electrical machine, power converters and techniques have been developed to control the real and reactive power of the induction machine, limit power output, control voltage and speed. There is lot of research going on around the world in this area and technology is being developed that offers great deal of capability. It requires an understanding of power systems, machines and applications of power electronic converters and control schemes put together on a common platform.

Wind energy has been the subject of much recent research and development. In order to overcome the problems associated with fixed speed wind turbine system and to maximize the wind energy capture, many new wind farms employ variable speed wind turbine. Double Fed Induction Generator (DFIG) is one of the components of variable speed wind turbine system.

DFIG offers several advantages when compared with fixed speed generators including speed control. These merits are primarily achieved via control of the rotor side converter. Many works have been proposed for studying the behaviour of DFIG based wind turbine system connected to the grid. Most existing models widely use vector control Double Fed Induction Generator. The stator is directly connected to the grid and the rotor is fed to magnetize the machine.

Doubly Fed Induction Generator is most popular variable speed WECS [2]. It has several benefits such as better efficiency, rating of the converter is less as the semiconductor converter units are connected with rotor circuit, cost efficient, minimum loss of converters, easy power factor correction, possibility of four quadrant active and reactive power controls and better utilization factor.

DFIG has 20-30% of more energy output than other variable speed WECS. And tip speed ratio is maintained at optimal due to rotor speed, i.e., it can be adjusted by proportion of low wind to moderate wind speeds.

In DFIG, the output terminal of stator is directly connected to the grid and slip power of rotor circuit is connected with grid through AC-DC and DC-AC power semiconductor converters. These converters are used to convert the slip power into rated values of DFIG. Both stator and rotor powers of DFIG are fed with grid and it shares the load [1].

Objectives: In view of the foregoing brief discussion, the objectives of the project are summarized as follows:

1. Modelling of a variable speed wind energy conversion system (WECS) including a doubly fed induction generator as an electrical power generation unit.
2. Investigating the performance of the DFIG under balanced condition.
3. Investigating the effect of the grid faults on the dynamic performance of variable speed wind-driven doubly fed induction generator connected to the grid.

The whole project is divided into 5 chapters:

Chapter 1 gives a brief description of DFIG and its advantages. The objectives of the project are also included in this chapter.

Chapter 2 contains the controlling of DFIG.

Chapter 3 contains the dynamic modelling of DFIG.

Chapter 4 contains the performance of DFIG during unbalanced grid condition.

Chapter 5 contains the Simulink model, simulation result and brief discussion.

Chapter 6 gives the conclusion.

CHAPTER 2

CONTROL OF DOUBLY FED INDUCTION GENERATOR (DFIG) DRIVEN BY A WIND TURBINE

The wind power system consists of a doubly fed induction generator (DFIG), where the stator winding is directly connected to the network and the rotor winding is connected to the network through a four quadrant power converter comprised of two back-to-back sinusoidal PWM. The thyristor converter can be used but they have limited performance. Usually, the controller of the rotor side converter regulates the electromagnetic torque and supplies part of the reactive power to maintain the magnetization of the machine [5]. On the other hand, the controller of the grid side converter regulates the DC link.

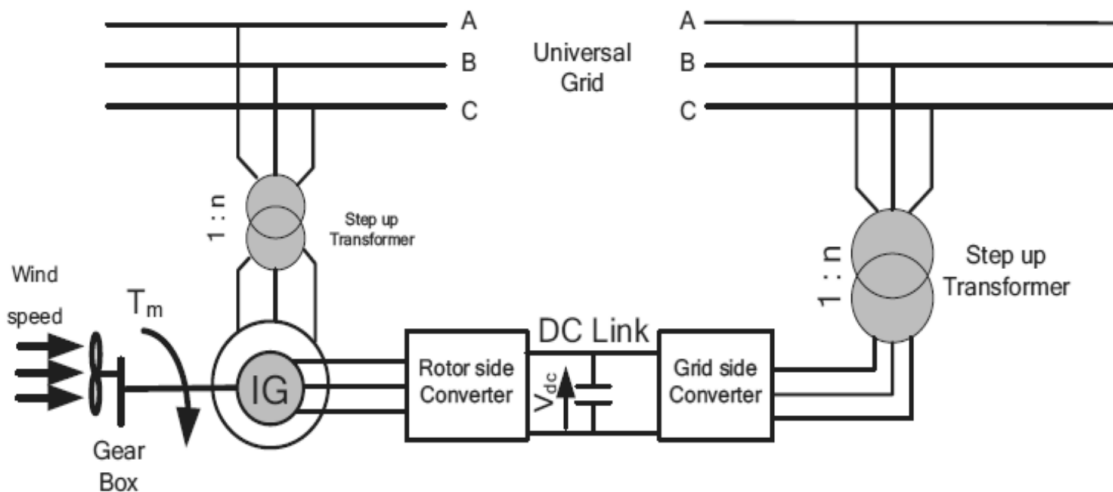


Figure 2.1 Doubly fed wound rotor induction generator driven by a wind turbine

2.1 Field Oriented Control of an Induction Machine

The control system of a variable speed wind turbine with DFIG has goals to control the reactive power interchanged between the generator and the grid and the active power drawn from the wind turbine in order to track the wind turbine optimum operation point or to limit the power in the case of high wind speeds. Each wind turbine system contains subsystems (aero dynamical, mechanical, electrical) with different ranges of time constants, i.e. the electrical dynamics are typically much faster than the mechanical. This difference in time constants becomes even bigger in the case of a variable speed wind turbine, due to the

presence of the power electronics. Such more complicated electrical system requires a more sophisticated control system too. The DFIG control system contains two decoupled control channels: one for the rotor side converter and one for the grid side converter. As the pulse-width modulation factor PWM is the control variable of the converter, each of these control channels generates a pulse-width modulation factor PWM, for the respective converter. This control variable is a complex number and therefore can control simultaneously two variables, such as the magnitude and phase angle of the rotor induced voltage. For example, for a predefined DC voltage and a control variable (pulse width modulation factor PWM), the line-to-line AC-voltage is determined. On the other hand, the wind turbine control is a control with slow dynamic responses. The wind turbine control contains two cross-coupled controllers: a torque controller and a power limitation controller. It supervises both the pitch angle actuator system of the wind turbine and the reactive power set point of the DFIG control level. It thus provides both a reference pitch angle β directly to the pitch actuator and a converter reference reactive power signal for the measurement grid point.

Nowadays many variable speed wind turbines (WT) are based on DFIGs, which are connected to the grid through back to back converters. The major advantage of these facilities lies in the fact that the power rate of the inverters is around the 25-30% of the nominal generator power. This feature permits to regulate the electrical power production within this range, something that has been proven to be a good trade-off between optimal operation and costs. The most used power control systems for DFIG-WTs are normally based on voltage oriented control (VOC) algorithms. The most extended version of such systems takes advantage of the field oriented control (FOC) principle. Regarding this method, an accurate synchronization with the stator flux vector enables to perform a decoupled control of the injection of active (P) and reactive (Q) powers, by means of the q and the d component of the rotor's currents in the Park's synchronous reference frame. From now on this FOC algorithm will be referenced as voltage oriented control in the synchronous reference frame (FOC-SRF) [7]. In addition to the decoupled control of P and Q, the synchronous reference frame transforms enables the FOCSRF to treat the state variables of the machine as continuous signals. This feature has launched its implementation in many DFIG-WTs, as the tuning of the controller parameters can be easily achieved.

The basic idea behind this control is to transform the three phase quantities in AC machine in an orthogonal d-q system aligned to one of the fluxes in the machine. Thus, a decoupling in controlling the flux and electromagnetic torque of the machine is achieved.

Two method of field oriented control for induction machine is used namely: indirect and direct field oriented control.

The indirect field oriented control can operate in four-quadrant down to standstill and it is widely used in motor drives and generator application. Typically the orthogonal synchronous reference frame is aligned on the rotor flux. However, this control is highly dependent on machine parameters.

The direct field control oriented along the stator flux does not need information about the rotor speed and is less sensitive to the machine parameters .However; it presents low performances for low speeds near to standstill.

A general control structure for field oriented control in synchronous reference frame for induction machines is shown in figure 2.2.

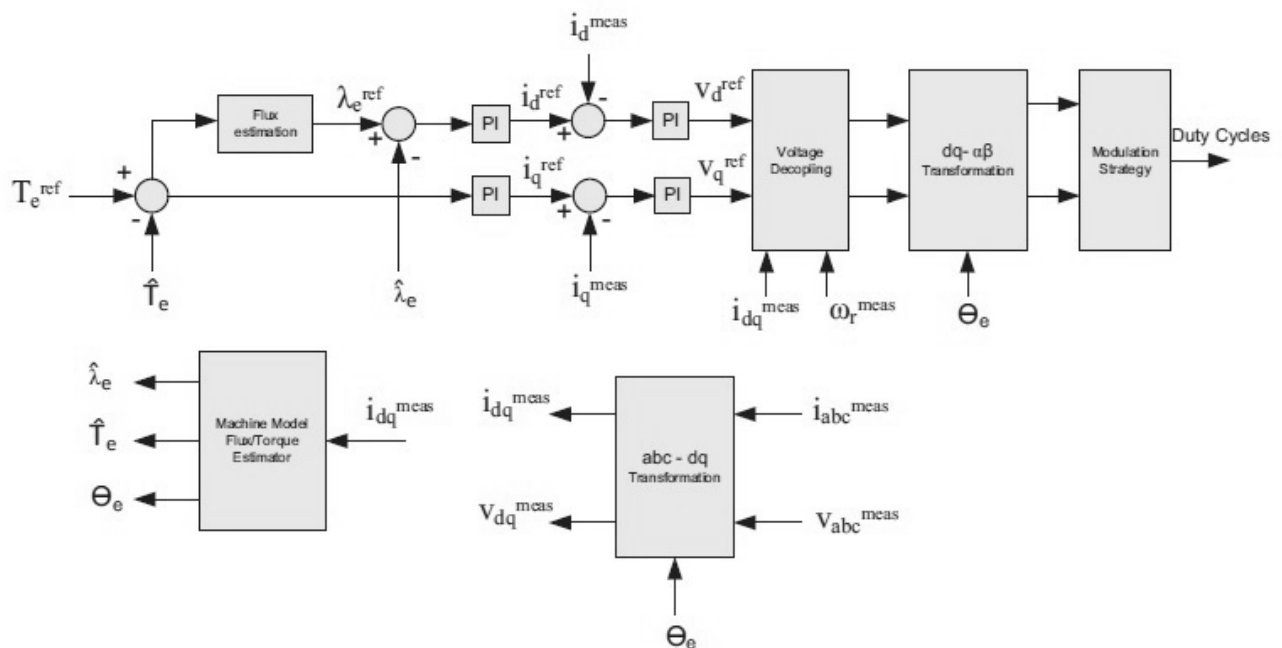


Figure 2.2 General structure of a field oriented control in a synchronous reference frame for an Induction machine.

The q-axis controls the electromagnetic torque while the d-axis controls the flux of the machine. The actual flux and torque as well as the flux angle are determined based on the machine equations using the currents. Similar control structure is used for the DFIG systems. Typically the outer control loops are used to regulate the active and reactive power on the stator side of the machine.

A comparison between the two basic schemes of field orientation can be made as following:

Direct Field Oriented control (DFO)

Indirect Field Oriented control (IFO)

Direct field orientation originally proposed by Blaschke, requires flux acquisition (position and magnitude) which is mostly obtained from computational techniques using machine terminal quantities. Whereas IFO avoids the direct flux acquisition, by adding an estimated and regulated slip frequency to the shaft speed and integrating the result to obtain the rotor flux position.

2.1.1 Direct Field Oriented Control of a Wind Driven DFIG

In DFO the position of the rotor flux, which is essential for the correct orientation, is directly measured using search coils as shown in figure 2.3 or estimated from terminal measurements. However using sensors to acquire the flux information makes it impossible to use off the shelf induction machine because installation of such sensors can be done only during machine manufacturing.

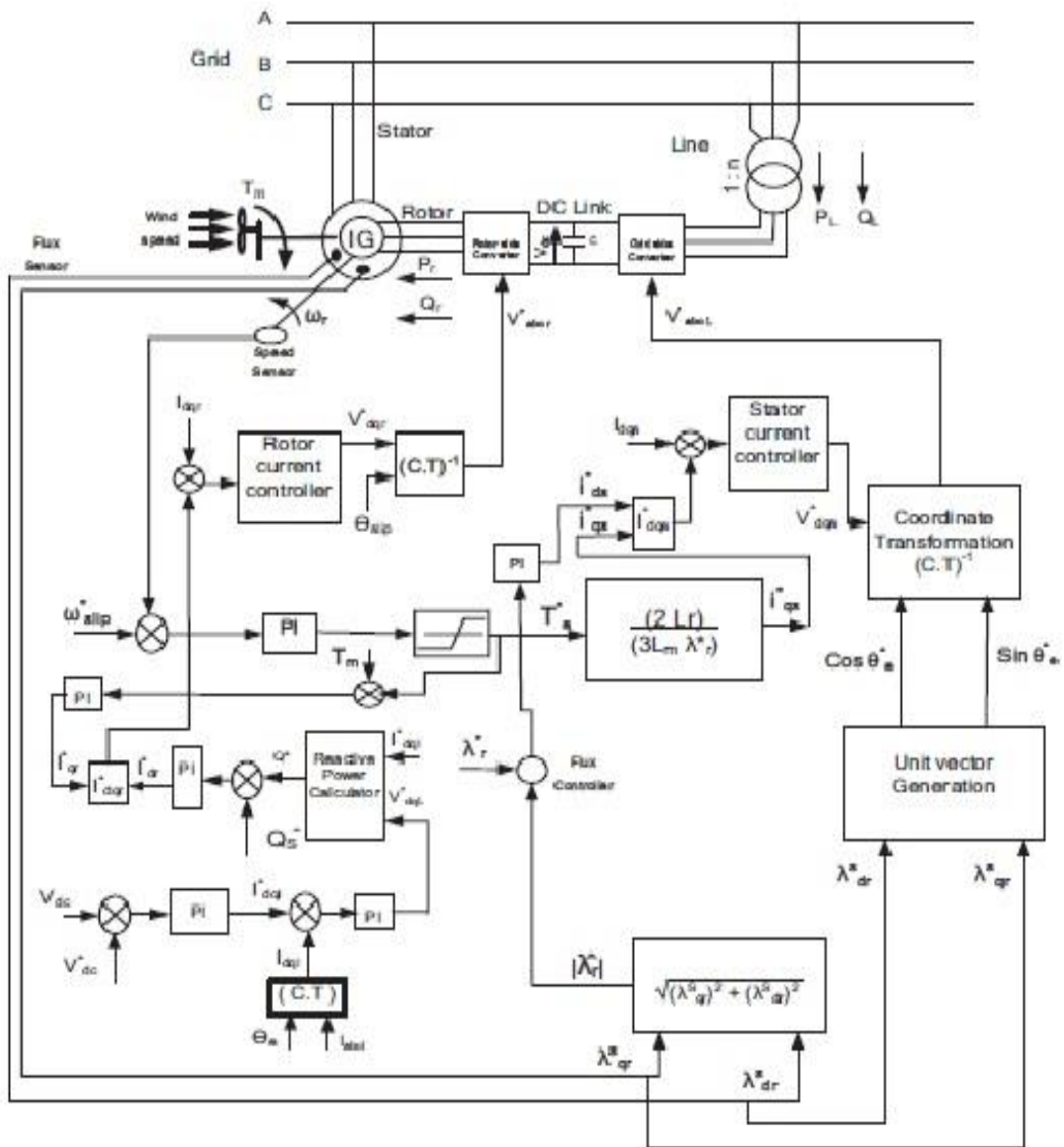


Figure 2.3 Structure of a direct field oriented control of a wind driven DFIG

CHAPTER 3

DYNAMIC MODELLING OF DFIG

3.1 Turbine model

To operate a wind turbine at its optimum operation condition at different wind speeds, the wind turbine should be operated at its maximum power coefficient ($C_p(\beta, \mu)_{\text{optimum}} = 0.3-0.5$) [6]. The wind turbine should be operated at a constant tip-speed ratio (μ) for operating around its maximum power coefficient. The aerodynamic power generated by wind turbine can be written as

$$P_m = 0.5 \rho A V_w^3 C_p(\beta, \mu) \quad (3.1)$$

Where the turbine power coefficient is defined in terms of the rotor blade tip speed (μ) and the blade pitch angle (β) as

$$C_p(\beta, \mu) = 0.73 \left(\frac{151}{\mu} - 0.002\beta - 13.2 \right) e^{-18.4/\mu}$$

Where $\mu = D_r \omega_r / 2 V_w$

At lower wind speed, the blade pitch angle (β) is set to a null value, because, the maximum power coefficient is obtained for this angle. Pitch angle control operates only when the value for wind speed is greater than the nominal wind speed.

To track the wind speed precisely, the wind turbine output power can also be expressed in terms of the rotor speed. In reality, the wind turbine rotor has a significantly large inertia due to the blade inertia and other rotating components.

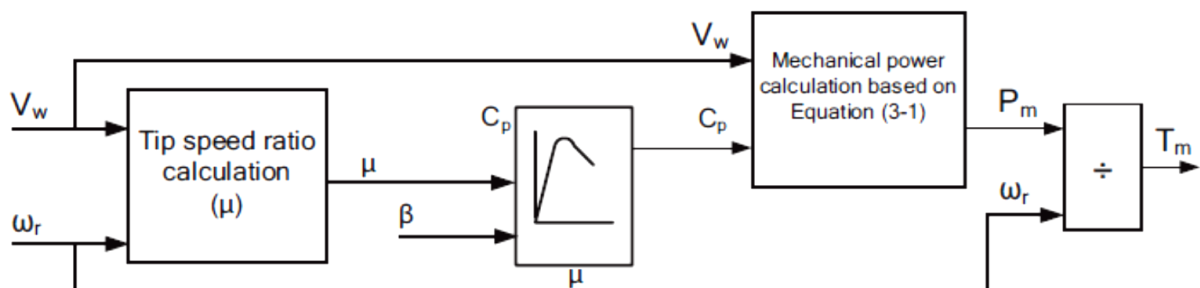


Figure 3.1 Wind turbine control system

Figure 3.1 shows the wind turbine control system, inputs to block are turbine speed (ω_r), blade pitch angle (β) and wind speed (V_w). The mechanical torque on the shaft is calculated as

$$T_m = P_m / \omega_r \quad (3.2)$$

The general equations for the d^s-q^s representation of an induction machine, in the stationary stator reference frame, are given as [6]

$$\begin{bmatrix} V_{ds}^s \\ V_{qs}^s \\ V_{dr}^s \\ V_{qr}^s \end{bmatrix} = \begin{bmatrix} R_s + pL_s & 0 & pL_m & 0 \\ 0 & R_s + pL_s & 0 & pL_m \\ pL_m & \omega_r L_m & R_r + pL_r & \omega_r L_r \\ -\omega_r L_m & pL_m & -\omega_r L_r & R_r + pL_r \end{bmatrix} \begin{bmatrix} i_{ds}^s \\ i_{qs}^s \\ i_{dr}^s \\ i_{qr}^s \end{bmatrix} \quad (3.3)$$

The developed electromagnetic torque can be expressed in terms of stator and rotor current components as:

$$T_e = \frac{3P}{2} \frac{L_m}{2} (i_{qs}^s i_{dr}^s - i_{ds}^s i_{qr}^s) \quad (3.4)$$

The mechanical equation in the generating region is given as:

$$T_m = J_m p\omega_r + B\omega_r + T_e \quad (3.5)$$

The state-space form of equation (3.5) can be written as:

$$p\omega_r = \frac{T_m - T_e - B\omega_r}{J_m} \quad (3.6)$$

3.2 DC link model

Figure 3.2 shows the blocked diagram of the dc link model, which consists of the line side and rotor side converters and the dc link capacitor. The dc link capacitor provides dc voltage to the grid side converter and any attempt to store active power in the capacitor would raise its voltage level [6]. To ensure stability of the system, power flow of the line side and rotor side converters, as indicated in figure 3.2, should guarantee the following control objective:

$$P_l = P_r \quad (3.7)$$

The differential equation of the dc link can be written as:

$$pCV_{dc} = i_1 - i_2 \quad (3.8)$$

Where V_{dc} is the dc voltage at the converter output terminals and C is the smoothing capacitor. Assuming no power losses for the converters, i_1 and i_2 can be derived as:

$$i_1 = P_l/V_{dc} \quad (3.9)$$

$$i_2 = P_r/V_{dc} \quad (3.10)$$

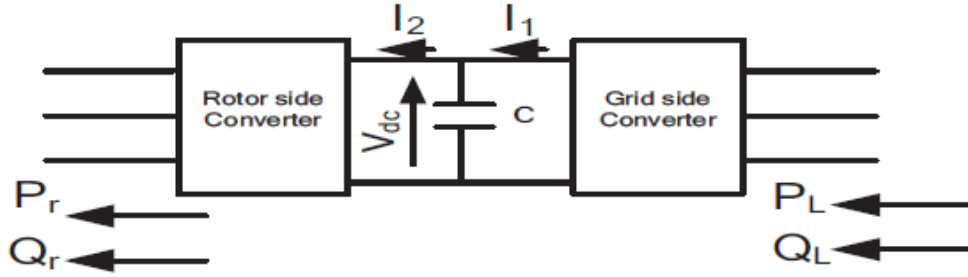


Figure 3.2 Power flow through dc-link element

3.3 Complete System Model

The above subsystem dynamic models can be interfaced to form the unified nonlinear dynamic model of the wind generation system [3]. The system can be described by the following differential equations:

$$pi_{ds}^s = A_2\omega_r L_m i_{qs}^s - R_s A_1 i_{ds}^s + R_r A_2 i_{dr}^s + A_1\omega_r L_m i_{qr}^s - A_1 V_{ds}^s \quad (3.11)$$

$$pi_{qs}^s = A_1 V_{qs}^s - R_s A_1 i_{qs}^s - A_2\omega_r L_m i_{ds}^s + R_r A_2 i_{qr}^s - A_1\omega_r L_r i_{dr}^s \quad (3.12)$$

$$pi_{dr}^s = -A_2\omega_r L_m i_{qs}^s + R_s A_2 i_{ds}^s - A_1\omega_r L_s i_{qr}^s - A_3 i_{dr}^s + A_2 V_{ds}^s \quad (3.13)$$

$$pi_{qr}^s = R_s A_2 i_{qs}^s + A_2\omega_r L_s i_{ds}^s - A_3 i_{qr}^s + A_1\omega_r L_s i_{dr}^s \quad (3.14)$$

$$\text{Where } A_1 = \frac{L_r}{(L_s L_r - L_m^2)}, A_2 = \frac{L_m}{(L_s L_r - L_m^2)}, \text{ and } A_3 = \frac{R_r(1 + A_2 L_m)}{L_r}$$

$$p\omega_r = \frac{1}{J_m} \left[T_m - B\omega_r - \frac{3P}{2} L_m (i_{qs}^s i_{dr}^s - i_{ds}^s i_{qr}^s) \right] \quad (3.15)$$

$$pCV_{dc} = \frac{P_l}{V_{dc}} - \frac{P_r}{V_{dc}} \quad (3.16)$$

3.4 Field Oriented Control of a DFIG

The field orientation techniques allow decoupled or independent control of both active and reactive power. These techniques are based on the concept of d^e-q^e controlling in different reference frames, where the current and the voltage are decomposed into distinct components related to the active and reactive power [8]. In this work, the stator flux oriented rotor current control, with decoupled control of active and reactive power is adopted for maximum power curve, for maximum power capturing and to be able to control the reactive power generation. These control objectives must be achieved with adequate stability of the system which also includes the power converter and the dc link. The total active and reactive power generated can be expressed in terms of d^e-q^e stator voltage and current components by the following equations:

$$P_s = \frac{3}{2} |V_s| i_{qs}^e \quad (3.17)$$

$$Q_s = \frac{3}{2} |V_s| i_{ds}^e \quad (3.18)$$

Where

$$|V_s| = \sqrt{(V_{ds}^e)^2 + (V_{qs}^e)^2}$$

The field orientation control is based on the field d^e-q^e model, where the reference frame rotates synchronously with respect to the stator flux linkage, with the d-axis of the reference frame instantaneously overlaps the axis of the stator flux. By aligning the stator flux phasor λ_s on the d^e – axis, so ($\omega = \omega_e$ and $\lambda_{qs}^e = 0$, $\lambda_{ds}^e = \lambda_s$). In such case the following expressions are obtained

$$\begin{aligned} \lambda_{qs}^e &= L_s i_{qs}^e + L_m i_{qr}^e = 0 \\ \therefore i_{qs}^e &= -\frac{L_m}{L_s} i_{qr}^e \end{aligned} \quad (3.19)$$

The developed electromagnetic torque can be expressed in terms of d^e-q^e stator current and flux components as:

$$T_e = \frac{3P}{2} (i_{qs}^e \lambda_{ds}^e - i_{ds}^e \lambda_{qs}^e) \quad (3.20)$$

By putting $\lambda_{qs}^e = 0$, in the torque equation, this yields:

$$\therefore T_e = \frac{3P}{2} (i_{qs}^e \lambda_{ds}^e) \quad (3.21)$$

Using (3.19) and the active power equation (3.17), the equation of the active power becomes:

$$P_s = -\frac{3}{2} |V_s| \frac{L_m}{L_s} i_{qr}^e \quad (3.22)$$

The d^e -axis stator current component can be written as:

$$i_{ds}^e = i_{md}^e - i_{dr}^e \quad (3.23)$$

Stator reactive power can be expressed as:

$$Q_s = \frac{3}{2} |V_s| \left(\frac{|V_s|}{2\pi f_s L_m} - i_{dr}^e \right) \quad (3.24)$$

Therefore, the d^e -axis rotor current component, (i_{dr}^e) can be obtained by regulating the stator reactive power. On the other hand, the q^e -axis rotor current component, (i_{qr}^e) can be obtained by controlling the generated torque which is obtained from the stator active power and the generator speed.

The stator flux linkage components in the stationary stator reference frame can be calculated through the integration of the difference between the phase voltage and the voltage drop in the stator resistance as:

$$\begin{aligned} \lambda_{ds}^s &= \int (V_{ds}^s - i_{ds}^s R_s) dt \\ \lambda_{qs}^s &= \int (V_{qs}^s - i_{qs}^s R_s) dt \end{aligned} \quad (3.25)$$

The magnitude of the stator flux linkage and its phase angle are given by,

$$\begin{aligned} \lambda_s &= \sqrt{(\lambda_{ds}^s)^2 + (\lambda_{qs}^s)^2} \\ \theta_e &= \tan^{-1} \frac{\lambda_{qs}^s}{\lambda_{ds}^s} \end{aligned} \quad (3.26)$$

3.5 Complete system configuration

Figure 3.3 shows the block diagram of the DFIG driven by a wind turbine control system. The control system consists of a reactive power controller, a torque controller, three current controllers, three co-ordinate transformations (C.T), two sinusoidal pulse-width modulation (SPWM) for transistor bridge inverters, a stator flux and torque estimators and reactive power calculator. The reference value of reactive power, Q_s^* , can be either directly implemented to the converter, considering the appropriate power, or calculated from equation (3.24).

Individual control of the rotor side converter (RSC) and of the grid side converter (GSC) and related feedback between the two converters are shown. A sinusoidal pulse width modulator (SPWM) provides field oriented currents i_{dr}^e and i_{qr}^e to the rotor circuit, controlling stator reactive power and electromagnetic torque respectively. The co-ordinate transformation voltage references by using the field angle.

The control inputs to the (SPWM) are the line voltage or rotor voltage commands and predefined triangular carrier waves. The SPWM modulator calculates the pulse pattern and supplies firing signals to the inverter. In the PWM scheme, the inverter output voltage is defined by the intersections of the voltage commands and carrier waves, which are synchronized such that the carrier frequency is an inter multiple of the frequency of voltage commands. This manner of synchronization eliminates sub harmonic generation.

The reference Torque is given by the turbine optimal torque-speed profile. Another (SPWM) is used to interface with the power network, possibly through a transformer. In the same d^e - q^e reference frame as determined by the stator flux, its currents (i_{ql}^e and i_{dl}^e) are also field oriented, controlling P_L and Q_L , respectively. As discussed earlier, P_L is controlled through i_{ql}^e to stabilize the dc bus voltage and Q_L is controlled through i_{dl}^e to meet the overall reactive power command.

The RSC controls the reactive power (Q) injection and the developed electric power (P_{elec}) by the DFIG. The electric power reference (P_{opt}^*) is determined based on the optimum rotor speed given by the C_p characteristic, depending on the wind speed as a parameter. The calculated reactive power of the DFIG (Q^*) is compared to the estimated one. The reference direct axis current (I_{dr}^{e*}) is then calculated from the resulting error, through a PI controller. I_{dr}^{e*} is then compared to the actual direct axis rotor current (i_{dr}^e), and the error is then sent to another PI controller to determine the reference value of the direct axis rotor voltage (V_{dr}^{e*}).

The quadrature axis component of the rotor current (I_{qr}^{e*}) is controlled in a similar manner as the direct axis component, regulates the developed electric power (P_{elec}) to an optimal reference (P_{opt}^*). The direct-quadrature components of the reference rotor voltages (V_{dr}^{e*} and V_{qr}^{e*}) are then transformed back into three-phase voltages (V_{abcr}^*), required at the RSC output, through a dq0-abc transformation. The converters IGBT's are considered to be ideal and commutation losses are therefore neglected.

The GSC controls the voltage level at the direct-current link (DC link). The line current (I_{dl}^e) is being calculated through a PI controller. I_{dl}^e is then compared to the actual value of the direct axis line current (I_{dl}) and then sent to another PI controller, in order to calculate the direct axis reference line voltage (V_{dl}^{e*}).

There is no need for a GSC reactive power regulation, since the RSC already controls the power factor of the DFIG. Therefore the quadrature axis component of the reference current is set to zero ($I_{ql}^{e*} = 0$). I_{ql}^{e*} is then compared to the quadrature axis component of the actual line current (I_{ql}) and the error is sent to a PI controller to determine the quadrature axis component of the reference line voltage (V_{ql}^{e*}). The two components of the reference line voltage (V_{dl}^{e*} and V_{ql}^{e*}) are then transformed into the three-phase voltages (V_{abcl}^*) needed at the output of the GSC.

The method uses stator reference frame model of the induction machine and the same reference frame is used in the implementation thereby avoiding the trigonometric operations encountered in the C.T of other reference frames. This is one of the advantages of the control scheme.

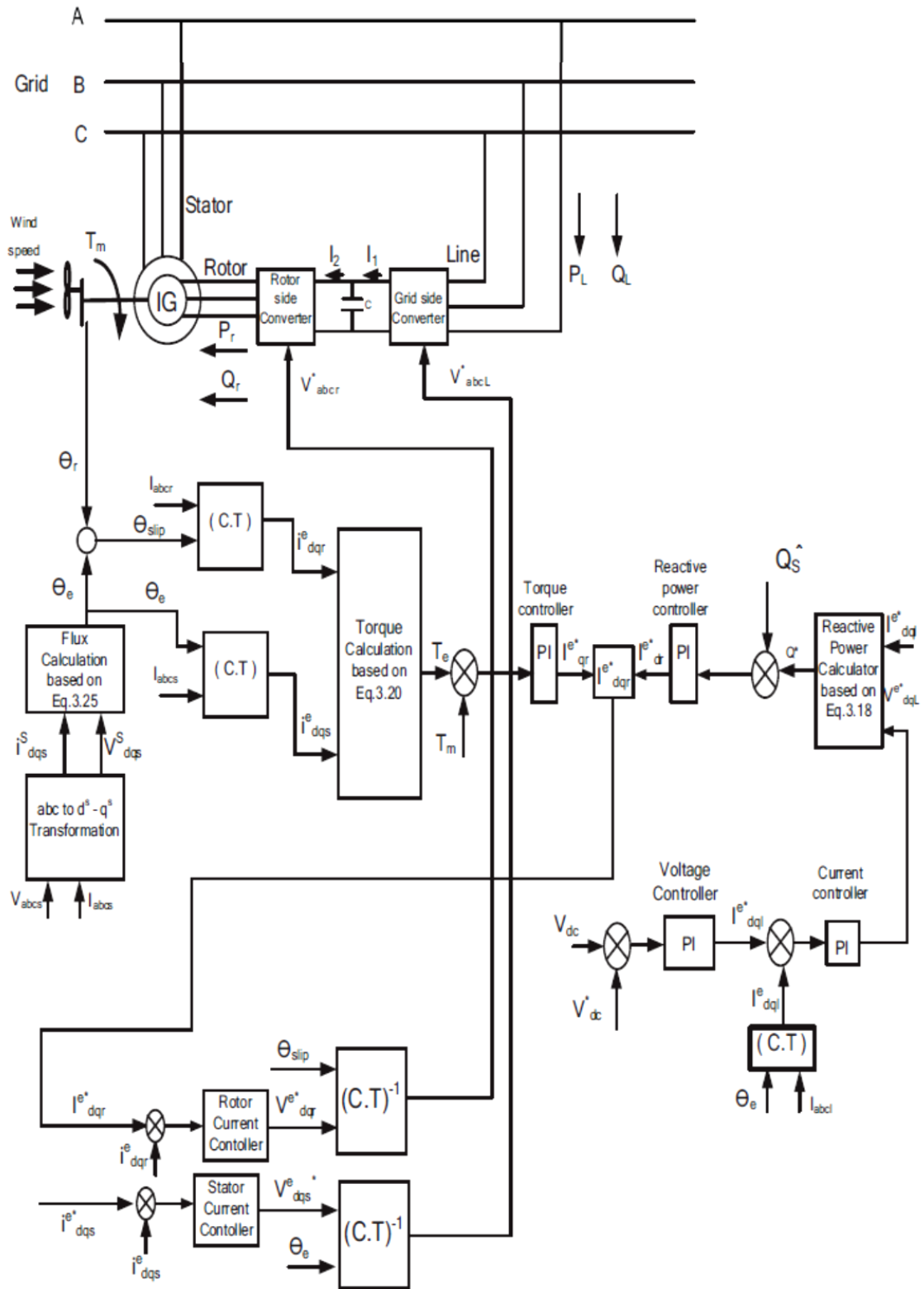


Figure 3.3 Control scheme of the DFIG driven by a wind turbine based on field orientation control

Table 3.1 Parameters and data specifications of the DFIG system.

$P_n(\text{nominal})$	$6 \times 1.5 = 9 \times 10^6$ MW
$V_n(\text{nominal})$	576 V
F_n	50 Hz
R_s	0.023 Ω
R_r	0.016 Ω
L_{ls}	0.18 H
L_{lr}	0.16 H
L_m	2.9 H
$V_{dc}(\text{nominal})$	1150 V
$H(s)$	0.685 sW/VA
B	0.00478 N.m./rad./s.
DC bus capacitor	10 mF
Nominal mechanical output power of wind turbine, at $V_w=15\text{m/s}$ and $\rho=1.25$ kg/m ² .	9×10^6 MW

3.6 Wind Power Model

For power system simulations involving grid disturbances, it is a reasonable approximation to assume that wind speed remains uniform for the 5 to 30 seconds typical of such cases. However, the mechanical power delivered to the shaft is complex function of wind speed, blade pitch angle and shaft speed. Further, with wind generation, the impact of wind power fluctuations on the output of the machines is of interest. The turbine model depends on the wind power model to provide this mapping [3].

The function of the wind power module is to compute the wind turbine mechanical power (shaft power) from the energy contained in the wind, using the following formula:

$$P = \frac{\rho}{2} A_r v_w^3 C_p(\lambda, \theta) \quad (3.27)$$

P is the mechanical power extracted from the wind, ρ is the air density in kg/m³, A_r is the area swept by the rotor blades in m², V_w is the wind speed in m/sec, and C_p is the power coefficient, which is a function of λ and θ . λ is the ratio of the rotor blade tip speed and the wind speed (V_{tip}/V_w), θ is the blade pitch angle in degrees. For the rigid shaft representation

used in this model, the relationship between blade tip speed and generator rotor speed, ω , is a fixed constant, K_b . The calculation of λ becomes:

$$\lambda = K_b (\omega/v_w) \quad (3.28)$$

Here, $K_b=56.6$ and $.5\rho A_r=0.00159$

C_p is a characteristic of the wind turbine and is usually provided as a set of curves relating C_p to λ , with θ as a parameter. Curve fitting was performed to obtain the mathematical representation of the C_p curves used in the model:

$$C_p(\theta, \lambda) = \sum_{i=0}^4 \sum_{j=0}^4 \alpha_{i,j} \theta^i \lambda^j \quad (3.29)$$

The coefficients $\alpha_{i,j}$ are given in Table 3.2. The curve fit is a good approximation for values of $2 < \lambda < 13$. Values of λ outside this range represent very high and low wind speeds, respectively, that are outside the continuous rating of the machine.

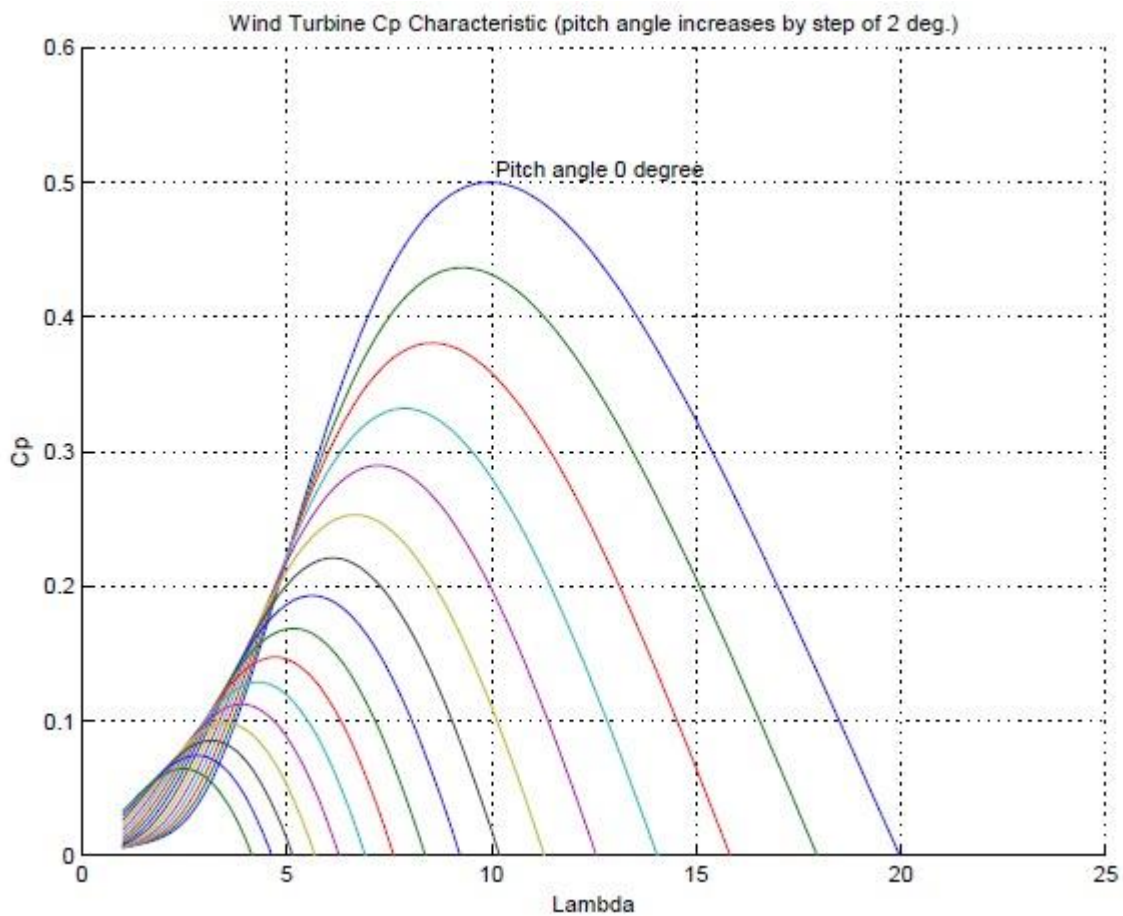


Figure 3.4 Wind Power C_p Curves

Initialization of the wind power model recognizes two distinct states: 1) initial electrical power (from the load flow) is less than rated, or 2) initial electrical power equal to rated. In either case, $P_{mech} = P_{elec}$ is known from the load flow and $\omega = \omega_{ref}$ is set at the corresponding value (1.2 pu if $P > 0.75$ pu). Then, using the C_p curve fit equation, the wind speed V_w required to produce P_{mech} with $\theta = \theta_{min}$ is determined. If P_{mech} is less than rated, this value of wind speed is used as the initial value. If P_{mech} is equal to rated and the user-input value of wind speed is greater than the $\theta = \theta_{min}$ value, then θ is increased to produce rated P at the specified value of wind speed.

Table 3.2 C_p coefficients $a_{i,j}$

i	j	a_{ij}
4	4	4.9686e-010
4	3	-7.1535e-008
4	2	1.6167e-006
4	1	-9.4839e-006
4	0	1.4787e-005
3	4	-8.9194e-008
3	3	5.9924e-006
3	2	-1.0479e-004
3	1	5.7051e-004
3	0	-8.6018e-004
2	4	2.7937e-006
2	3	-1.4855e-004
2	2	2.1495e-003
2	1	-1.0996e-002
2	0	1.5727e-002
1	4	-2.3895e-005
1	3	1.0683e-003
1	2	-1.3934e-002
1	1	6.0405e-002
1	0	-6.7606e-002
0	4	1.1524e-005
0	3	-1.3365e-004
0	2	-1.2406e-002
0	1	2.1808e-001
0	0	-4.1909e-001

CHAPTER 4

DYNAMIC PERFORMANCE OF DFIG DURING UNBALANCED GRID CONDITION

Unbalance may be defined as in several views, it can be voltage dip (also the word voltage sag is used) is a sudden reduction (between 10% and 90%) of the voltage at a point in the electrical system, and sudden change of load (dynamic load) .There can be many causes for a voltage dip: short circuits somewhere in the grid, switching operations associated with a temporary disconnection of a supply, the flow of the heavy currents which are caused by the start of large motor loads, or large currents drawn by arc furnaces or by transformer saturation. The magnitude of a voltage dip at a certain point in the system depends mainly on the type of the fault, the distance to the fault, the system configuration, and the fault impedance. As a result the effect of the fault is consequently transferred to the connected generator with the unbalanced grid. So the performance of the DFIG is also affected during the fault period.

This chapter describes the dynamic behaviour of a DFIG, operating with the wind turbine during unbalanced grid condition. The method of symmetrical components gives an elegant way of analysing the operation of a DFIG system during unbalanced conditions [7]. In the synchronous rotating flux-oriented positive and negative (d-q) reference frames, the mathematical model of a DFIG system under unbalanced supply is developed. Based on the developed model, the relationships between the electromagnetic torque, active and reactive powers, and the positive and negative sequence components of the stator flux and rotor current components are fully established.

4.1 Dynamic model of a DFIG system

The equivalent circuit of a DFIG can be expressed in the synchronous rotating reference frame as shown in figure 4.1. In this circuit the core losses and saturation are neglected.

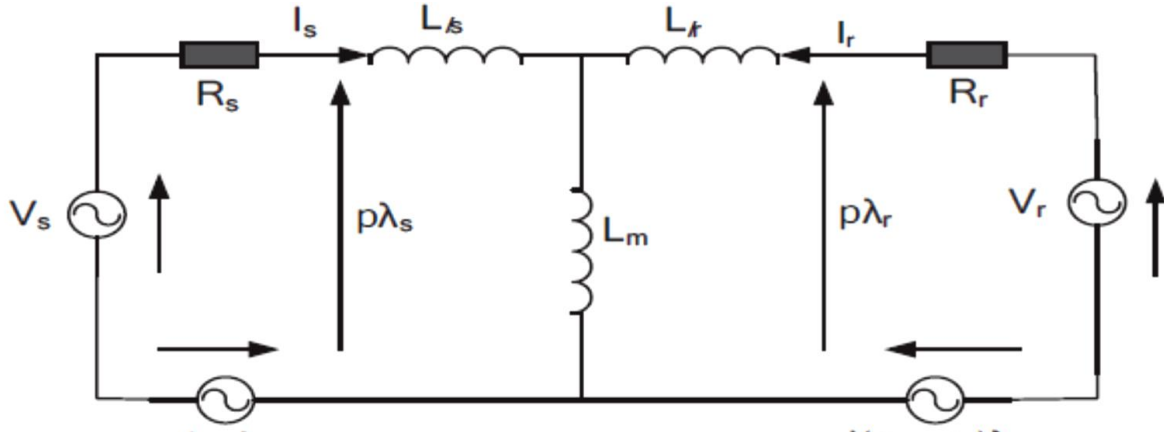


Figure 4.1 Equivalent circuit of a DFIG in the synchronous reference frame rotating at a speed of ω_s

According to figure 4.1, the stator and rotor flux linkages (λ_s and λ_r) are given, respectively by,

$$\begin{aligned} \lambda_s &= L_s I_s + L_m I_r \\ \lambda_r &= L_r I_r + L_m I_s \end{aligned} \quad (4.1)$$

Also, from this figure, the stator and rotor voltages V_s and V_r in the synchronous rotating reference frame can be expressed as:

$$V_s = R_s I_s + p\lambda_s + j\omega_s \lambda_s \quad (4.2)$$

$$V_r = R_r I_r + p\lambda_r + j(\omega_s - \omega_r) \lambda_r \quad (4.3)$$

Equation (4.1) can be rewritten for obtaining the rotor flux and stator current as:

$$\lambda_r = \frac{L_m}{L_s} \lambda_s + \sigma L_r I_r \quad (4.4)$$

$$I_s = \frac{1}{L_s} (\lambda_s - L_m I_r) \quad (4.5)$$

Where, $\sigma = 1 - L_m^2 / (L_s L_r)$ is the leakage factor.

Substituting equations (4.4) and (4.5) into equation (4.3), this yields

$$V_r = R_r I_r + \sigma L_r p I_r + \frac{L_m}{L_s} p \lambda_s + j(\omega_s - \omega_r) (\sigma L_r I_r + \frac{L_m}{L_s} \lambda_s) \quad (4.6)$$

As the stator voltage is usually constant, which results in constant stator flux, equation (4.6) can be simplified as:

$$V_r = R_r I_r + \sigma L_r p I_r + j(\omega_s - \omega_r) (\sigma L_r I_r + \frac{L_m}{L_s} \lambda_s) \quad (4.7)$$

Separating the real and imaginary parts of equation (4.7) into d-q components, the rotor voltage equation can be expressed in state space form as:

$$p \begin{bmatrix} I_{dr} \\ I_{qr} \end{bmatrix} = \begin{bmatrix} -R_r/(\sigma L_r) & (\omega_s - \omega_r) \\ -(\omega_s - \omega_r) & -R_r/(\sigma L_r) \end{bmatrix} \begin{bmatrix} I_{dr} \\ I_{qr} \end{bmatrix} + \frac{(\omega_s - \omega_r)L_m}{\sigma L_r L_s} \begin{bmatrix} \lambda_{qs} \\ -\lambda_{ds} \end{bmatrix} + \frac{1}{\sigma L_r} \begin{bmatrix} V_{dr} \\ V_{qr} \end{bmatrix} \quad (4.8)$$

Using equations (4.2) and (4.5), and after neglecting the effect of stator voltage drop ($R_s I_s$), the stator output active and reactive powers can be calculated as:

$$\begin{aligned} P_s + jQ_s &= -\frac{3}{2} \vec{V}_s \times \vec{I}_s \approx -\frac{3}{2} j\omega_s \lambda_s \times \frac{1}{L_s} (\lambda_s - L_m \vec{I}_r) \\ &= -\frac{3}{2} \omega_s (j\lambda_s) \times \frac{1}{L_s} [(\lambda_s - L_m I_{dr}) + j L_m I_{qr}] \\ &= \frac{3}{2} \frac{\omega_s}{L_s} [\lambda_s L_m I_{qr} - j \lambda_s (\lambda_s - L_m I_{dr})] \end{aligned} \quad (4.9)$$

Thus, the stator active and reactive powers in terms of (d-q) rotor current components and stator flux are given by,

$$\begin{aligned} P_s &= \frac{3}{2} \frac{\omega_s}{L_s} \lambda_s L_m I_{qr} \\ Q_s &= -\frac{3}{2} \frac{\omega_s}{L_s} \lambda_s (\lambda_s - L_m I_{dr}) \end{aligned} \quad (4.10)$$

4.2 Mathematical Model of DFIG System Under Unbalanced Grid Voltage

The unbalanced three-phase quantities such as voltage, current, and flux may be decomposed into positive and negative sequence components, assuming no zero sequence components [7]. In the stationary (α - β) reference frame, the voltage, current, and flux can be decomposed into positive and negative sequence components as,

$$\begin{aligned} F_{\alpha\beta}(t) &= F_{\alpha\beta+}(t) + F_{\alpha\beta-}(t) \\ &= |F_{\alpha\beta+}| \cdot e^{-j(\omega_s t + \phi^+)} + |F_{\alpha\beta-}| \cdot e^{-j(\omega_s t + \phi^-)} \end{aligned} \quad (4.11)$$

Where ϕ^+ and ϕ^- are the respective phase shift for positive and negative sequence components and F represents the voltage, current, or flux vector.

Figure 4.2 shows that, for the positive (d-q)⁺ reference frame, the d⁺ axis is fixed to the positive stator flux rotating at the speed of ω_s . While for the negative (d-q)⁻ reference frames, as can be seen from figure 4.2, its d⁻ axis rotates at an angular speed of $-\omega_s$ with the phase angle to the α -axis being $-\theta_s$.

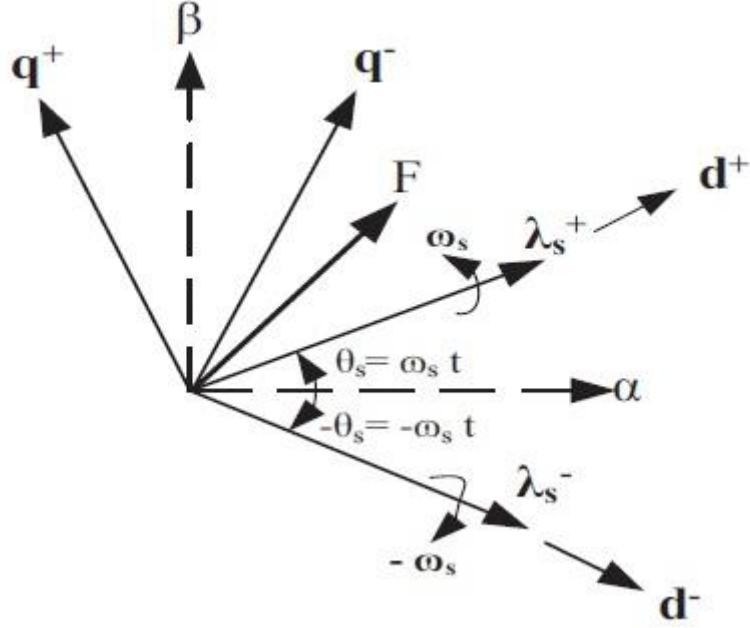


Figure.4.2. Relationships between the $(\alpha\text{-}\beta)$ reference frame and the $(d\text{-}q)^+$ and $(d\text{-}q)^-$ reference frames.

From figure.4.2, the transformation from $(\alpha\text{-}\beta)$ reference frame to $(d\text{-}q)^+$ and $(d\text{-}q)^-$ reference frames are given by,

$$F_{dq}^+ = F_{\alpha\beta} \cdot e^{j\omega_s t} = F_{dq}^- \cdot e^{+j2\omega_s t} \quad (4.12)$$

$$F_{dq}^- = F_{\alpha\beta} \cdot e^{-j\omega_s t} = F_{dq}^+ \cdot e^{j-2\omega_s t} \quad (4.13)$$

Similar to grid connected converters, during network unbalance, the state space form of the rotor model given in equation (4.8) can be expressed in the positive and negative sequence components, rotating at angular frequency of ω_s and $-\omega_s$, respectively as:

$$p \begin{bmatrix} I_{dr}^+ \\ I_{qr}^+ \end{bmatrix} = \begin{bmatrix} -R_r/(\sigma L_r) & (\omega_s - \omega_r) \\ -(\omega_s - \omega_r) & -R_r/(\sigma L_r) \end{bmatrix} \begin{bmatrix} I_{dr}^+ \\ I_{qr}^+ \end{bmatrix} + \frac{L_m (\omega_s - \omega_r)}{\sigma L_r L_s} \begin{bmatrix} \lambda_{qs}^+ \\ -\lambda_{ds}^+ \end{bmatrix} + \frac{1}{\sigma L_r} \begin{bmatrix} V_{dr}^+ \\ V_{qr}^+ \end{bmatrix} \quad (4.14)$$

$$p \begin{bmatrix} I_{dr}^- \\ I_{qr}^- \end{bmatrix} = \begin{bmatrix} -R_r/(\sigma L_r) & (-\omega_s - \omega_r) \\ -(-\omega_s - \omega_r) & -R_r/(\sigma L_r) \end{bmatrix} \begin{bmatrix} I_{dr}^- \\ I_{qr}^- \end{bmatrix} + \frac{L_m (-\omega_s - \omega_r)}{\sigma L_r L_s} \begin{bmatrix} \lambda_{qs}^- \\ -\lambda_{ds}^- \end{bmatrix} + \frac{1}{\sigma L_r} \begin{bmatrix} V_{dr}^- \\ V_{qr}^- \end{bmatrix} \quad (4.15)$$

According to figure.4.2 and equations (4-11), (4-12), and (4-13), the stator and rotor current and voltage vectors can be expressed using their respective positive and negative sequence components as:

$$V_{dqs} = V_{dqs}^+ + V_{dqs}^- \cdot e^{-j2\omega_s t} \quad (4.16)$$

$$V_{dqr} = V_{dqr}^+ + V_{dqr}^- \cdot e^{-j2\omega_s t} \quad (4.17)$$

Although unbalanced, the stator voltage can still be regarded as being constant. Therefore,

$$p \lambda_{dqs}^+ = 0, p \lambda_{dqs}^- = 0 \quad (4.18)$$

Under unbalanced network conditions, the amplitude and rotating speed of the stator flux are no longer constant. Neglecting the stator resistance and taking into account equations (4.2), (4.4), (4.5), (4.16) and (4.17), the stator voltage and current can be expressed in the positive (d-q)⁺ reference frame as:

$$\vec{V}_{dqs} = j\omega_s (\lambda_{dqs}^+ + \lambda_{dqs}^- \cdot e^{-j2\omega_s t}) \quad (4.19)$$

$$\vec{I}_{dqs} = \frac{1}{L_s} (\lambda_{dqs}^+ + \lambda_{dqs}^- \cdot e^{-j2\omega_s t}) - \frac{L_m}{L_s} (I_{dqr}^+ + I_{dqr}^- \cdot e^{-j2\omega_s t}) \quad (4.20)$$

Similar to balanced condition, the stator output active and reactive powers can be calculated as:

$$P_s + jQ_s = -\frac{3}{2} \vec{V}_{dqs} \times \vec{I}_{dqs} \quad (4.21)$$

Substituting (4.19) and (4.20) into (4.21) and separating the active and reactive power into different oscillating components yield,

$$\begin{aligned} P_s &= P_{s0} + P_{s \sin 2} \cdot \sin(2\omega_s t) + P_{s \cos 2} \cdot \cos(2\omega_s t) \\ Q_s &= Q_{s0} + Q_{s \sin 2} \cdot \sin(2\omega_s t) + Q_{s \cos 2} \cdot \cos(2\omega_s t) \end{aligned} \quad (4.22)$$

Where,

$$\begin{aligned} P_{s0} &= \frac{3 L_m \omega_s}{2 L_s} [-\lambda_{qs}^+ I_{dr}^+ + \lambda_{ds}^+ I_{qr}^+ + \lambda_{qs}^- I_{dr}^- - \lambda_{ds}^- I_{qr}^-], \\ Q_{s0} &= \frac{3 \omega_s}{2 L_s} [-\lambda_{ds}^{+2} - \lambda_{qs}^{+2} + \lambda_{ds}^{-2} + \lambda_{qs}^{-2}] + \frac{3 L_m \omega_s}{2 L_s} [\lambda_{ds}^+ I_{dr}^+ + \lambda_{qs}^+ I_{qr}^+ \\ &\quad - \lambda_{ds}^- I_{dr}^- - \lambda_{qs}^- I_{qr}^-], \end{aligned}$$

$$P_s \sin 2 = \frac{3 \omega_s}{2L_s} [\lambda_{ds}^- \lambda_{ds}^+ + \lambda_{qs}^- \lambda_{qs}^+ + \lambda_{ds}^+ \lambda_{ds}^- + \lambda_{qs}^+ \lambda_{qs}^-] \\ + \frac{3 L_m \omega_s}{2L_s} [-\lambda_{ds}^- I_{dr}^+ - \lambda_{qs}^+ I_{qr}^+ - \lambda_{ds}^+ I_{dr}^- - \lambda_{qs}^- I_{qr}^-],$$

$$P_s \cos 2 = \frac{3 \omega_s}{2L_s} [-\lambda_{qs}^- \lambda_{ds}^+ + \lambda_{ds}^- \lambda_{qs}^+ + \lambda_{qs}^+ \lambda_{ds}^- - \lambda_{ds}^+ \lambda_{qs}^-] \\ + \frac{3 L_m \omega_s}{2L_s} [\lambda_{qs}^- I_{dr}^+ - \lambda_{ds}^- I_{qr}^+ - \lambda_{qs}^+ I_{dr}^- + \lambda_{ds}^+ I_{qr}^-],$$

$$Q_s \sin 2 = \frac{3 L_m \omega_s}{2L_s} [\lambda_{qs}^- I_{dr}^+ - \lambda_{ds}^- I_{qr}^+ + \lambda_{qs}^+ I_{dr}^- - \lambda_{ds}^+ I_{qr}^-],$$

$$Q_s \cos 2 = \frac{3 L_m \omega_s}{2L_s} [-\lambda_{ds}^- I_{dr}^+ - \lambda_{qs}^- I_{qr}^+ + \lambda_{ds}^+ I_{dr}^- + \lambda_{qs}^+ I_{qr}^-],$$

According to figure.4.1, the electromagnetic power equals to the sum of the power outputs from the equivalent voltage source $j\omega_s\lambda_s$ and $j(\omega_s-\omega_r)\lambda_s$. Thus, it is given by,

$$P_e = \frac{-3}{2} \text{Re}[j\omega_s \vec{\lambda}_{dqs}^+ \times \vec{I}_{dqs}^+ + j(\omega_s - \omega_r) \vec{\lambda}_{dqr}^+ \times \vec{I}_{dqr}^+] \\ = \frac{-3}{2} \text{Re} \left[j\omega_s \vec{\lambda}_{dqs}^+ \times \frac{1}{L_s} (\vec{\lambda}_{dqs}^+ - L_m \vec{I}_{dqr}^+) \right] \\ - \frac{3}{2} \text{Re}[j(\omega_s - \omega_r) (\frac{L_m}{L_s} \vec{\lambda}_{dqs}^+ + \sigma L_r \vec{I}_{dqr}^+) \times \vec{I}_{dqr}^+] \\ = \frac{3 L_m}{2 L_s} \omega_r \text{Re}[j \vec{\lambda}_{dqs}^+ \times \vec{I}_{dqr}^+] = P_{e0} + P_{e \sin 2} + P_{e \cos 2} \quad (4.23)$$

Where,

$$\begin{bmatrix} P_{e0} \\ P_{e \sin 2} \\ P_{e \cos 2} \end{bmatrix} = \frac{3 L_m}{2 L_s} \omega_r \begin{bmatrix} -\lambda_{qs}^+ & \lambda_{ds}^+ & -\lambda_{qs}^- & \lambda_{ds}^- \\ \lambda_{ds}^- & \lambda_{qs}^- & -\lambda_{ds}^+ & -\lambda_{qs}^+ \\ -\lambda_{qs}^- & \lambda_{ds}^- & -\lambda_{qs}^+ & \lambda_{ds}^+ \end{bmatrix} \begin{bmatrix} I_{dr}^+ \\ I_{qr}^+ \\ I_{dr}^- \\ I_{qr}^- \end{bmatrix}$$

The electromagnetic torque of the DFIG is calculated as:

$$T_e = \frac{P_e}{\omega_r} = (P_{e0} + P_{e \sin 2} + P_{e \cos 2})/\omega_r \quad (4.24)$$

4.3 System Description

Figure 4.3 shows a basic layout of a single line diagram for a DFIG driven by a wind turbine system during grid fault conditions. The machine may be simulated as an induction machine having 3-phase unbalanced supply voltages in the stator and in the rotor. The method of symmetrical components is used for analysing this simulated machine for obtaining the stator and rotor current and voltage components. In this figure, the method of a field orientation is used for controlling the stator and rotor currents and voltages to allow decoupling or independent control of both active and reactive powers. Fault across the grid terminals have been studied to investigate the dynamic response in the DFIG's performance during the fault period [1].

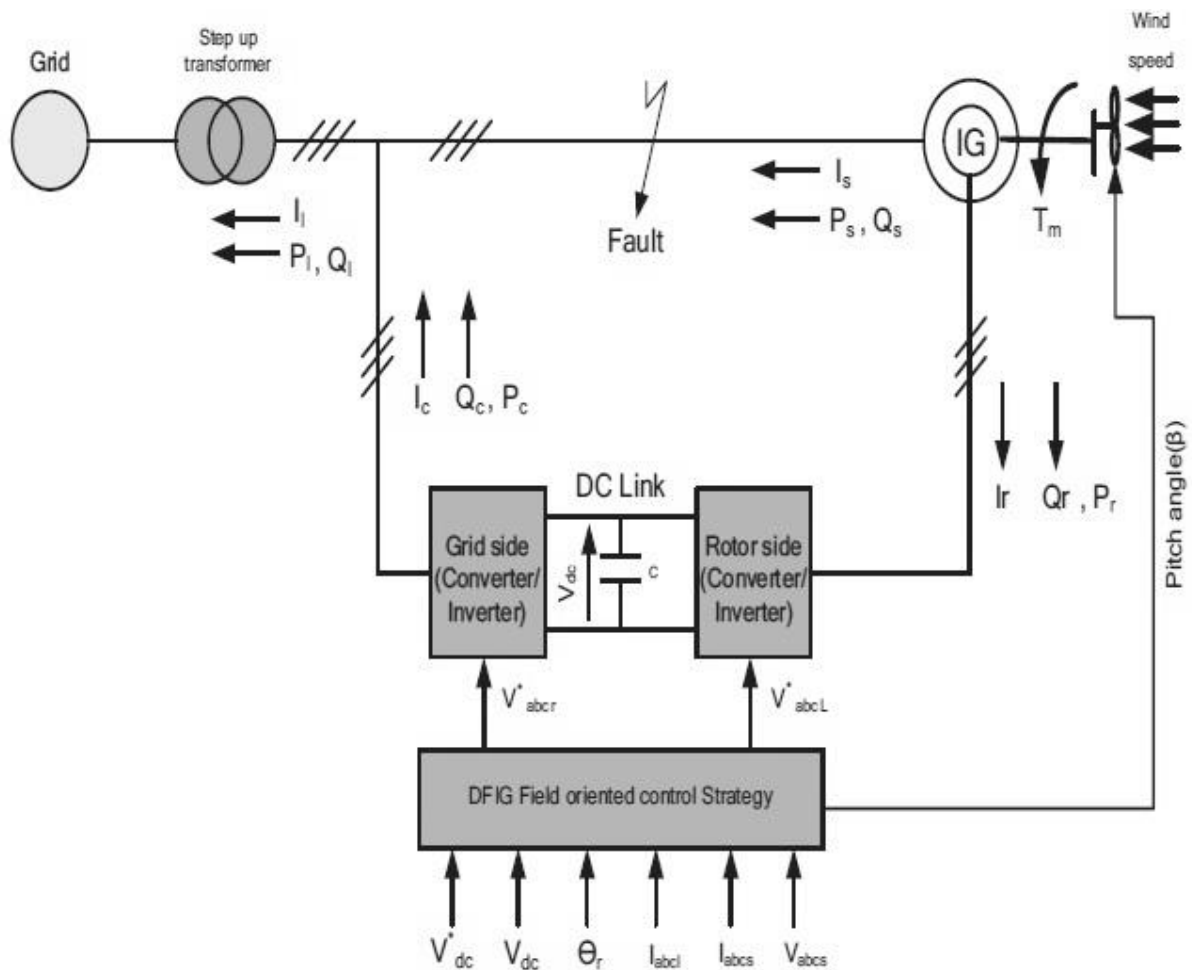


Figure 4.3 DFIG driven by a wind turbine based on field orientation control during grid fault conditions

CHAPTER 5

SIMULINK MODEL, SIMULATION RESULTS AND DISCUSSION

5.1 Simulink model

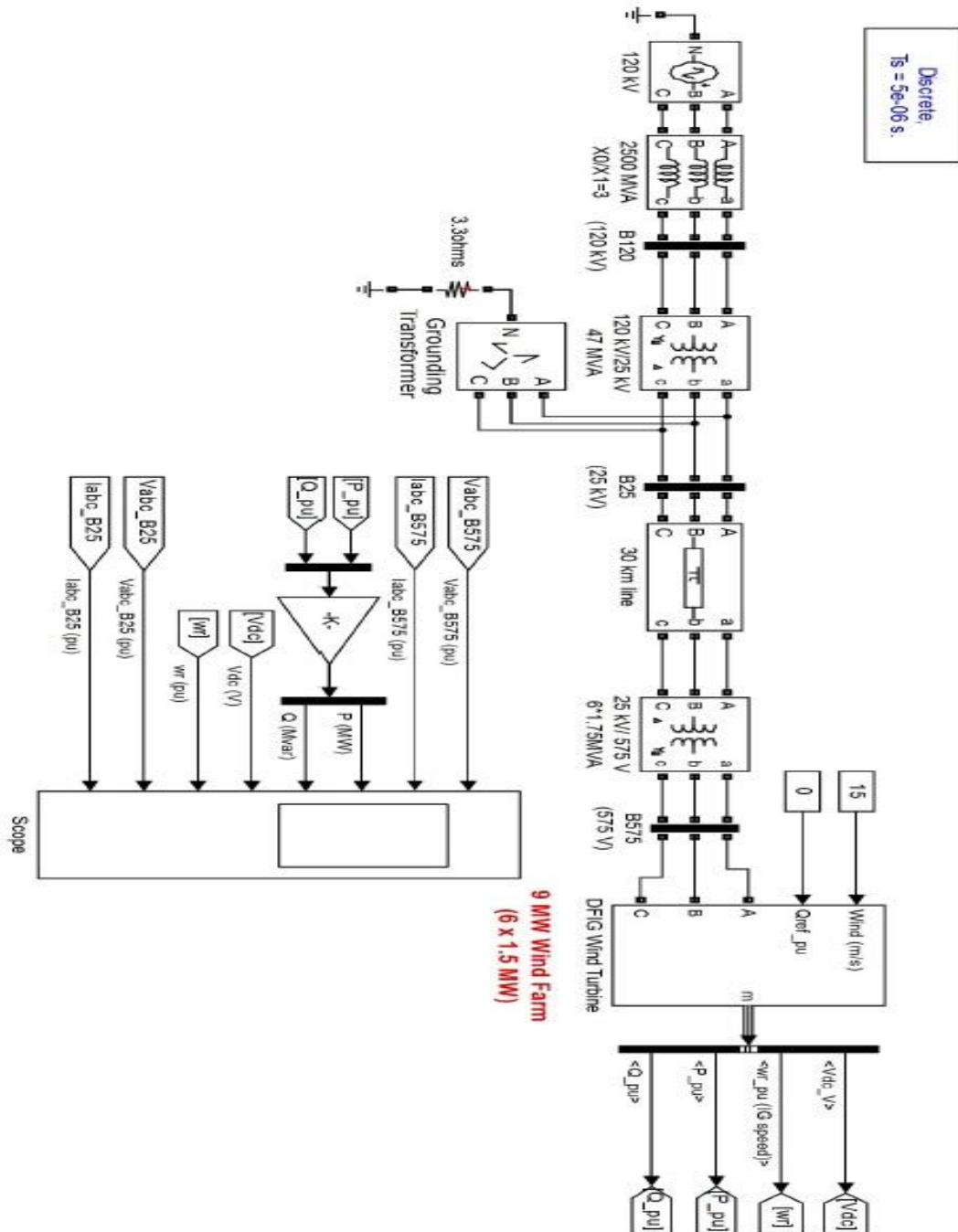


Figure 5.1 Simulink model for normal operation of the DFIG system

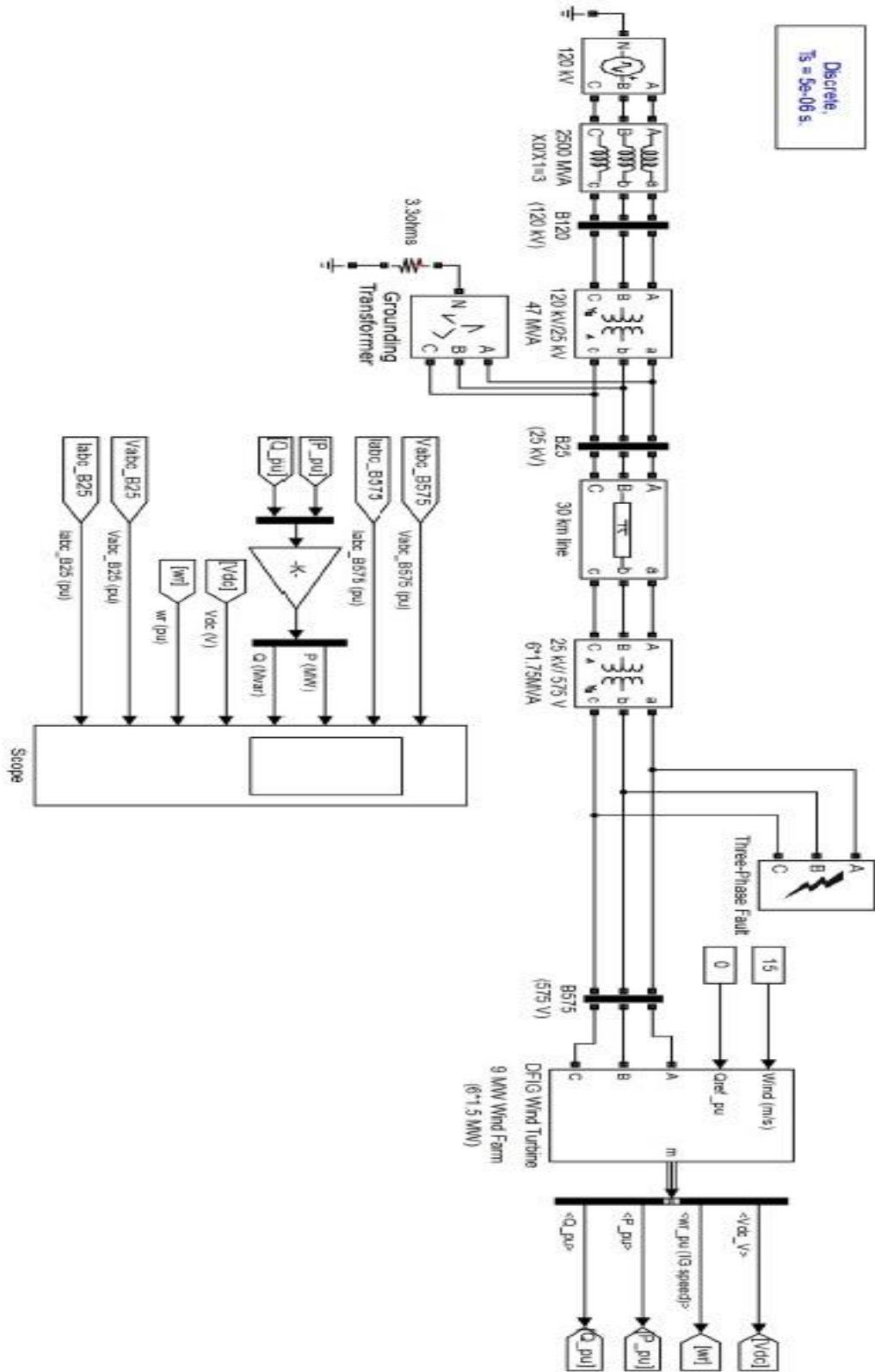


Figure 5.2 Simulink model of DFIG system during unbalanced network condition

5.2 Results and Discussion

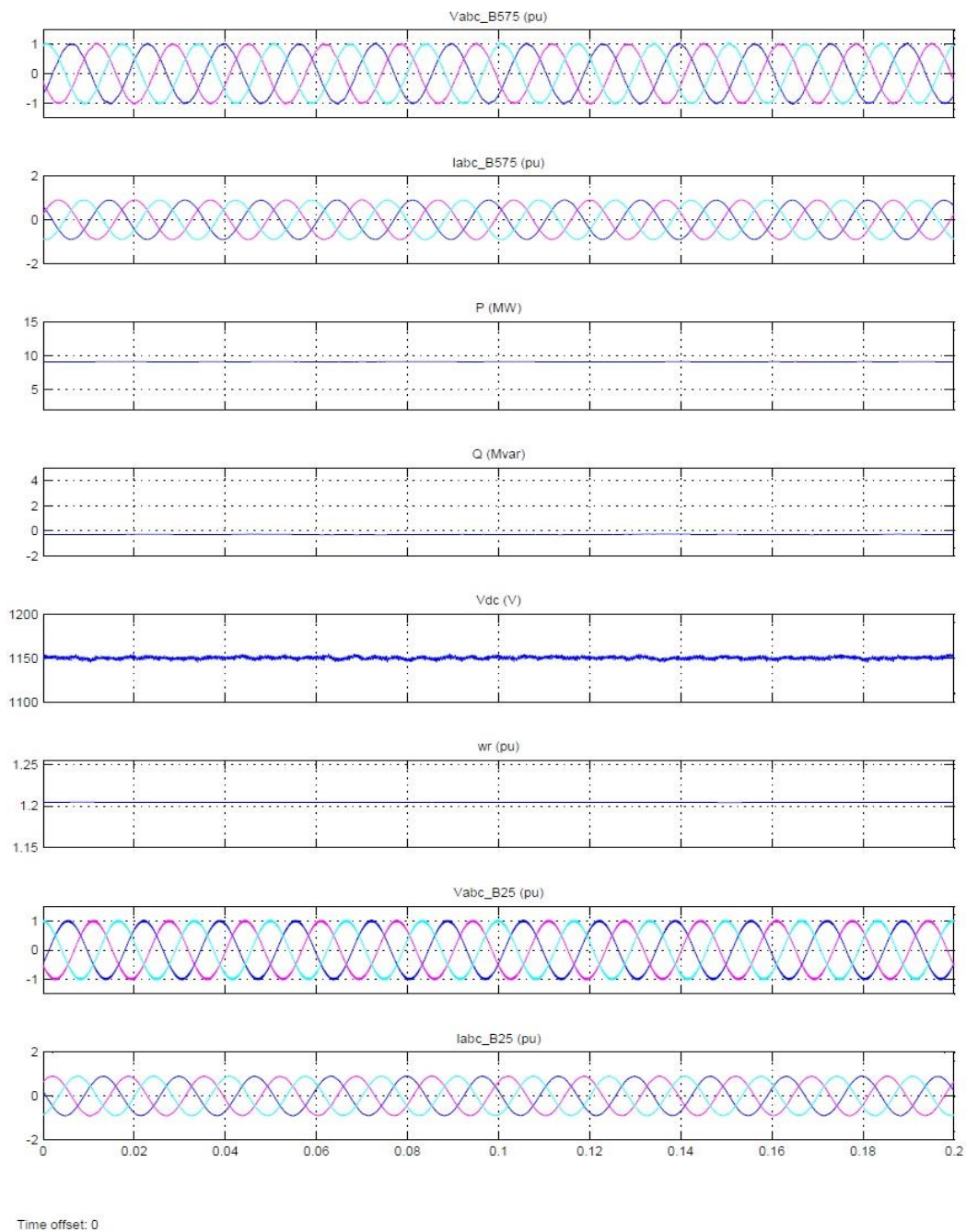
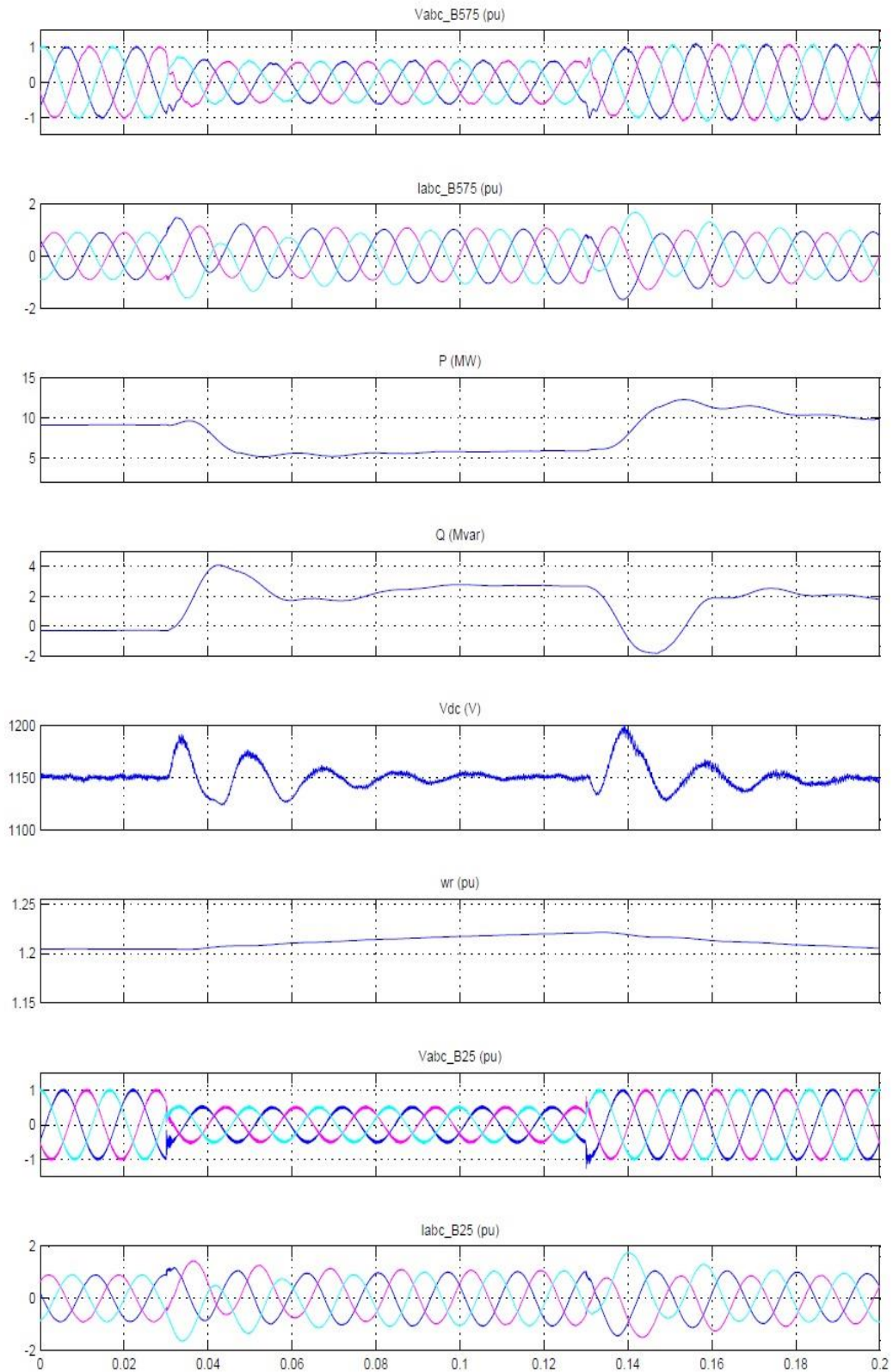


Figure 5.3 Simulation result under normal operation

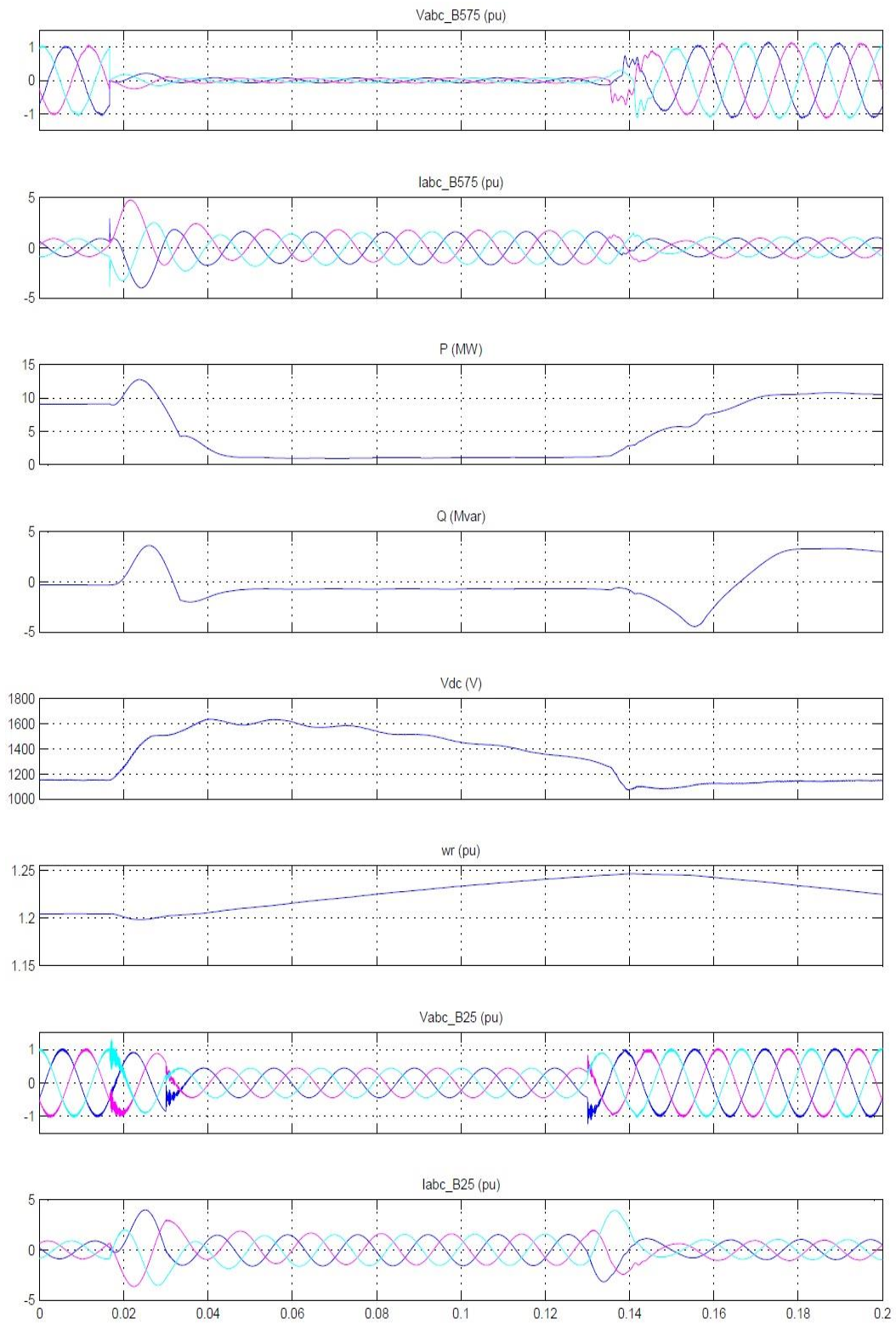
Figure 5.3 shows the simulation result under normal operation. Here it is seen that the bus voltage and current are maintaining fine sinusoidal wave. The DFIG wind farm produces 9 MW. The turbine speed is 1.2 pu of generator synchronous speed. The DC voltage is regulated at 1150V and reactive power is kept at 0 MVar. The active and reactive powers supplied by the utility grid are decoupled and DC link voltage is maintained constant due to the control strategy made in the GSC.



Time offset: 0

Figure 5.4 Simulation result during voltage sag

Figure 5.4 shows the simulation result during voltage sag. Here the steady state operation of the DFIG and its dynamic response to voltage sag resulting from a remote fault on the 120 kv system has been observed. At $t=0.03s$ the positive-sequence voltage suddenly drops to 0.05 pu causing an oscillation on the DC bus voltage and on the DFIG output power. From this figure it can be noticed that the generated active power is negatively affected and its value decreases by 44%. On the other hand the generated reactive power increases by 40%. The DC link voltage increases by about 3.5% of its normal value. The turbine speed increases the normal value. During the voltage sag the control system tries to regulate DC voltage and reactive power at their set points.



Time offset: 0

Figure 5.5 Simulation result during three phase fault

A three phase to ground fault is applied to the grid terminals. Figure 5.5 illustrates the harmful effect of the fault on the generated active and reactive powers respectively. From the figure it can be noticed that the value of generated active power reduces significantly by a percentage of 90% of its normal value, while the generated reactive power presents an increase of 5 times of its normal value during the fault period. Also, the effect of fault is appeared clearly on the dc link voltage which introduces a noticeable increase of 35% of its normal value due to the high values of line and rotor currents. All three phase voltages have been dropped to a very low value. It is noticed that their values have not been dropped to zero but they have a very low values but not equal zero. The reason for this is the existence of some leakage and coupling capacitance to ground in addition to the resistance of the grounding wires. It is noticed that the values of the three phase currents are increased during the fault period to about 4 times of their normal values.

CHAPTER 6

CONCLUSION

The project is performed to investigate the performance of the wind driven doubly fed induction generator under balanced and unbalanced grid network condition. The modelling, control and simulation of DFIG coupled with a wind turbine has been carried out. From the simulation results, it can be noticed that during the voltage sag the control system tries to regulate DC voltage and reactive power at their set points. During fault it is seen that there is an abrupt increase in DC link voltage and reactive power and consecutively the active power decreases to almost zero. Unbalanced grid voltages can cause many problems for DFIG wind turbines such as torque pulsations, unbalanced currents, and reactive power pulsations. These problems may be attributed to the instability in the power converter's DC link voltage during system disturbances. So, new techniques like FRT scheme or crow bar protection scheme are to be adopted to enhance the performance of the wind driven DFIG during unbalanced network condition.

REFERENCES

- [1] Mossa Mohmoud A, Modelling, Analysis and Enhancement of the performance of a Wind Driven DFIG During steady state and transient conditions. Hamburg, Anchor Academic Publishing, 2014.
- [2] C. Badrul H and C. Srinivas, "Double-fed induction generator control for variable speed wind power generation" *Electric Power Systems Research*, (2006) , Vol. 76, pp. 786-800.
- [3] L.M. Fernandez, C.A. Garcia and J.R. Saenz, "Aggregated dynamic model for wind farms with doubly fed induction generator wind turbines", *Renewable Energy*, (2008), Vol. 33, No .1, pp. 129–140.
- [4] E. Muljadi and C.P. Butterfield, "Pitch-controlled variable speed wind turbine generation", *IEEE Trans. Ind. Appl.* (2001), Vol. 37, No .1, pp. 240-246.
- [5] R. S. Pena, J. C. Clare and G. M. Asher, "Doubly fed induction generator using back-to-back PWM converters and its application to variable-speed wind-energy generation", *IEE Proc. Electric Power Applications*, (1996), Vol. 143, No. 3, pp. 231-341.
- [6] A. Tapia, G. Tapia, J.X. Ostolaza and J.R. Senz, "Modeling and control of a wind turbine driven doubly fed induction generator," *IEEE Trans. on Energy Conversion*, (2003), Vol. 18, pp.194-204.
- [7] Lie Xu , "Coordinated control of DFIG's rotor and grid side converters during network unbalance" *IEEE Trans. Power Electronics*, MAY (2008), Vol. 23, No. 3, pp.1041-1049.
- [8] B. Atkinson , D. Lakin, R. A and Hopfensperger , "Stator flux oriented control of a cascaded doubly-fed induction machine", *IEE Proc. Electr. Power Appl.* (Nov1999), Vol. 146, No. 6, pp.597–605.